Optics Letters

Vibrational modes in an optically levitated droplet

Xin Luo,[1] Zhihao Zhou,[1] Wei Liu,[2] Dongyi Shen,[2] Hengzhe Yan,[1] Yiqiao Lin,[1] and Wenjie Wan[1,2,*]

[1]MOE Key Laboratory for Laser Plasmas and Collaborative Innovation Center of IFSA, University of Michigan-Shanghai Jiao Tong University Joint Institute, Shanghai Jiao Tong University, Shanghai 200240, China
[2]The State Key Laboratory of Advanced Optical Communication Systems and Networks, Department of Physics and Astronomy, Shanghai Jiao Tong University, Shanghai 200240, China
*Corresponding author: wenjie.wan@sjtu.edu.cn

Received 24 June 2021; revised 20 August 2021; accepted 23 August 2021; posted 23 August 2021 (Doc. ID 434930); published 13 September 2021

Levitation by optical tweezers provides a unique non-invasive tool for investigating a microscale object without external perturbations. Here we experimentally levitate a micrometer-sized water droplet in the air using an optical tweezer. Meanwhile, vibrational modes of a levitated water droplet are excited by modulating the trapping laser. From their backscattered light, vibrational modes with mode numbers are observed in the spectra. Additionally, their corresponding free spectral ranges are analyzed and compared with theory and numerical simulations. This Letter, establishing a non-invasive and all-optical detection technique of optomechanical properties of levitated droplets, paves the way for their practical applications in aerosol and biomedical science.

https://doi.org/10.1364/OL.434930

Optical tweezers, from the pioneering work of Ashkin [1,2], have become an indispensable tool to capture and detect micro-objects with the advantages of non-contact and high precision operation capabilities, which promotes significant progress in physical science, molecular biology, and many other fields [3–5]. In the biology field, optical tweezers allow manipulating and interrogating molecules and cells, such as measuring the movement of a motor protein kinesin [6], trapping a chain of yeast cells [7], and obtaining information about cell strain ability [8]. In material science, optical tweezers not only permit the self-assembly of nanoparticles, but also enable the nano-processing technology by trapped particles with nanometer-level accuracy [9]. In these applications, however, the trapped particles are mostly realized in liquid environments. Levitating a micrometer-sized object in the air by optical tweezers is a challenging task due to the stability problem from airflow [10], but it is also an important technique to isolate the object from direct contact like thermal/electrical conduction, or other external perturbation [11], such that many important properties at the gas–liquid interface, e.g., surface tension, Kelvin effect [12], capillary resonances [13], vibrational modes [14–16], can be studied.

Among them, the vibrational modes of micrometer-sized droplets are of particular importance in the field of spray coating [17], inkjet printing [18], and microfluidic chips [19]. Droplet vibration also plays an important role in the droplet atomization process and can be applied to control the small-scale mixing/demixing of fluids and as a tool for measuring the surface tension and viscosity of sessile or levitated droplets [20]. However, prior studies are almost disturbed by the external substrates or supporting structures. For example, an atomic force microscope with a high vibration frequency has been utilized to drive the vibrations of a droplet for analyzing the vibration frequency, but this contact measurement destroys the surface properties by introducing a solid liquid interface [21]. Recently, a Michelson interferometry non-invasively enables observing the surface thermal vibrations of a liquid droplet, but still adhered to an optical fiber tip [22]. Meanwhile, optics provides another alternative and convenient way to excite optomechanical modes, including capillary [13], breathing [23], and Brillouin resonances [24] in liquid droplets, solid microstructures [25–27], and a liquid–solid hybrid environment [28,29]. In this way, if combined with the optical levitation technique, we may obtain an all-optical method, e.g., optical excitation and optical detection, through a tapered fiber coupler [25–29], to study the intrinsic properties of droplets, such as surface tension, viscosity, and density, in a non-invasive and non-destructive manner.

In this Letter, we experimentally observe vibrational modes of a levitated water droplet using an optical tweezer in the free space, where a near-infrared fiber laser (1064 nm) with the modulated intensity provides both a levitation force for the droplet and a time-varying force to excite the internal vibrational modes. Using this technique, water droplets with a diameter ranging from 8 to 13 μm have been successfully trapped and levitated in the air. From their backscattered light, vibrational modes with different mode numbers are observed in the spectrum. Additionally, their free spectral ranges are analyzed with respect to the diameters. These experimental observations have also been compared with theoretical and numerical calculations. This Letter opens up a new avenue for non-invasive detection of optomechanical modes and paves the way for their practice applications in aerosol and biomedical science.

Droplet levitation can be realized in our experimental configuration (Fig. 1) using a confocal microscope setup with two input lasers: 1064 nm laser beam and 532 nm laser beam. The

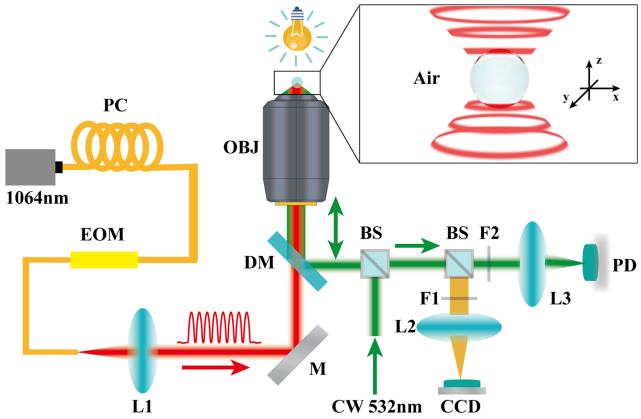

Fig. 1. Schematic diagram of the experimental levitation setup. An EOM modulates the intensity of a 1064 nm laser beam (NKT Photonics, Koheras BoostiK Y10), whose polarization is modified by a polarization controller (PC). Lens L1 represents a beam expander system (two lenses with focal length: 80 and 150 mm), making the spot size of 1064 nm laser beam slightly larger than the posterior pupil of the objective (OBJ). The 532 nm continuous wave (CW) reflected with a DM is coaxial with the modulated 1064 nm beam passing through DM (900 nm short-pass). The OBJ (Nikon LU Plan Fluor 100× NA 0.9) converges the two laser beams along the vertical axis (z axis) and collects the 532 nm backscattering light carrying the information of the vibrational modes. The beam splitter (BS) separates the detection system and image system. The imaging system includes a filter F1 blocking 532 nm and L2 representing two lenses with focal lengths 175 and 100 mm, while the detection system includes a filter F2 blocking part 1064 nm reflected by a DM and L3 with focal length 35 mm converging the 532 nm backscattering light on a photodetector (PD). The vibrational mode signal detected by the PD (APD 120 A/M Thorlabs) (APD 120A/M Thorlabs) is amplified by a lock-in amplifier (SR865A 4 MHz DSP Lock-in Amplifier) and stored by an oscilloscope for the subsequent analysis. The top right figure shows that the 1064 nm laser beam with color representing the light intensity from 0 to 300 mW captures a water droplet and excites the vibrational modes of a droplet in the air.

long-wavelength (1064 nm) laser beam creates the optical trap to levitate a single water droplet with an 8-13 μm diameter in the air. In the meantime, this 1064 nm laser with an average power of ∼300 mW is modulated by an electro-optical modulator (EOM) to excite the vibrational modes of the trapped droplet. The secondary 532 nm laser is launched to the droplet, and its backscattering light is measured by a photodiode with a lock-in amplifier linked to an oscilloscope for the subsequent analysis. Additionally, a filter F2 (950 nm short-pass filter) blocks the 1064 nm laser beam partly reflected by a dichroic mirror (DM). At the same time, a collimated parallel white light from a halogen lamp illuminates the levitated droplet, so we can obtain the shape information by a CCD camera (QHY5L-II-C) while a filter F1 (notch filter) blocks the 532 nm laser beam. Such a two-laser configuration enables us to capture a water droplet in the air and probe its vibrational modes in an all-optical manner.

To trap and levitate water droplets, we purposely design a double-deck vessel to slow down the speed of water mist and optically trap droplets, similar to prior works [30]. The water mist is ejected from an ultrasonic atomizer into the upper deck of the vessel, where the droplets slow down after collision and fusion and finally fall down to the bottom deck of the vessel. In this regime, a single droplet can successfully be trapped at

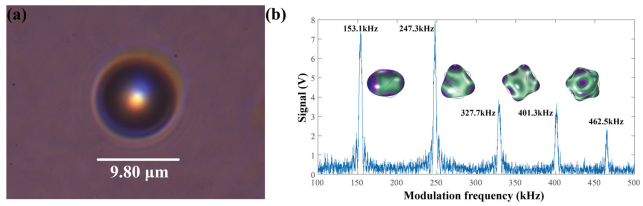

Fig. 2. (a) Levitated water droplet with a diameter of about 9.80 μm. (b) Output signal of the lock-in amplifier reveals the vibrational resonance frequencies of the droplet as 153.1, 247.3, 327.7, 401.3, and 462.5 kHz. These resonances are confirmed by the numerical simulations, and their corresponding capillary standing waves are depicted in the inset.

the laser focus within minutes. The objective lens to focus the laser is placed on a three-dimensional translational stage with a 100 nm resolution, which can be utilized to measure the size of the trapped droplets. To calibrate the imaging system, we record the position of a sample movement by the 3D translational stage and calculate the displacement to be around 6.28 μm per 100 pixels in the camera. After capturing a water droplet of a diameter ∼9.8 μm [Fig. 2(a)], we start to modulate the 1064 nm laser and sweep the modulation frequency from 100 to 500 kHz. From the backscattering 532 nm light, serval resonance modes ranging from 153.1 to 462.5 kHz are clearly presented in the spectrum [Fig. 2(b)]. Their corresponding resonance amplitudes decline with increasing frequency; in the meantime, the resonance Q factors change from 35 (at 153.1 kHz) to 197 (at 462.5 kHz). These resonances depict the vibrational modes with different mode orders of the trapped droplet.

Vibrational modes in liquid droplets can mainly be caused by a bulk modulus or surface tension as the restoring forces. The former one introducing compression force is responsible for acoustic waves trapped internally in the droplets with a frequency spanning from 100 MHz up to 10 GHz [24,31], similar to their counterpart in solid microstructures [25–27]. The latter case with surface tension can be interpreted as capillary vibrational resonances [13] with a much lower resonance frequency ∼kHz. We believe our experimental observations belong to this type. This capillary wave is highly sensitive to the liquid–air interface, offering a unique way to study such interface problems.

To understand the nature of experimental observed vibrational resonance modes, we perform numerical simulations using a finite element method [32,33]. Here we purposely design the two geometric-layer structure, separating the surface layer from the internal layer, where the surface layer is of 0.4 μm thickness, and the internal layer is with the diameter ranging from 6.8 to 12.8 μm. We set the bulk modulus of the internal layer to the bulk modulus of water: 1.62 $\mathrm{N/m^2} \times 10^9\ \mathrm{N/m^2}$, while setting the bulk modulus of the surface layer to γ/r, where γ is the tension coefficient of water (0.072 N/m), and r is the radius of the droplets; effectively, this equation transforms the surface tension coefficient to the bulk modulus [31]. In this manner, we can find these vibrational modes of the droplet to be capillary standing waves on the surface causing internal deformation. The first mode with a shape like a flat ellipsoid has two peaks and troughs, and the higher-order modes have more peaks and troughs [Fig. 2(b)]. These vibrational modes should satisfy the wall boundary condition and the periodic boundary condition.

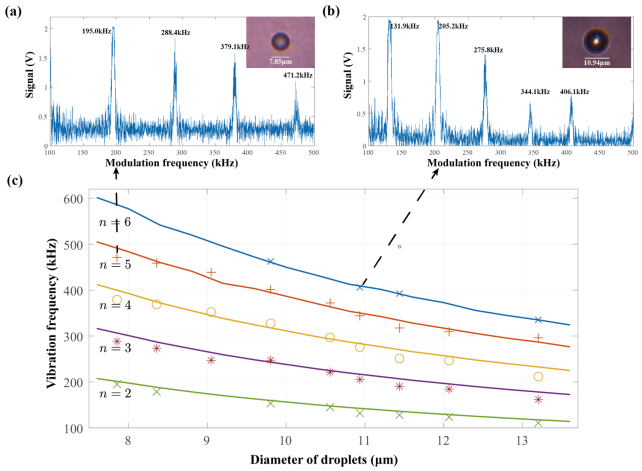

Fig. 3. (a) and (b) Vibrational resonance spectra of two levitated droplets with a diameter of about 7.85 and 10.94 μm. (c) Relationship curves between the droplet diameter, resonance mode number, and vibrational frequency. The solid lines with different colors are different vibrational modes in the simulation for the droplet with a diameter ranging from 7.6 to 13.6 μm. Additionally, these points are measured experimental data.

For the theoretical analysis, Sharp proposed a formula based on the standing wave, in which he assumed that the vibration of the droplet was regarded as the transmission of the droplet surface wave satisfied for the standing wave condition on the droplet and the transmission law of the wave [14,15]. Thus, the profile length of the droplet is equal to a half-integer number of wavelengths. Using the dispersion properties of the wave [16], the Sharp formula can be obtained as follows:

$$f_n = \frac{\alpha\pi}{2}\sqrt{\frac{n^3\gamma}{8\pi\rho R^3\theta^3}}, \tag{1}$$

where θ, R, ρ, γ, and n are the contact angle, radius, density, surface tension coefficient, and an integer representing the resonant mode (half-integer number) $n = 2, 3, 4, \ldots$, respectively. Additionally, α is a correction coefficient of the formula for the simplifying assumption of a droplet with a finite size. When the contact angle θ is equal to π, the droplet will be an isolated droplet and the frequency $f_n = \frac{\alpha}{2\pi}\sqrt{n^3\gamma/8\rho R^3}$. The Sharp formula states that the resonant frequency of the isolated droplet is inversely proportional to $R^{\frac{3}{2}}$.

To justify this theory, we levitate many water droplets of different sizes, excite their vibrational modes, and record their associated resonance frequencies in Fig. 3. Figures 3(a) and 3(b) show two typical resonance spectra of two levitated droplets with a diameter of about 7.85 and 10.94 μm. Obviously, the free spectral range (difference between two adjacent resonances) is enlarged with the smaller 7.85 μm droplet. Furthermore, droplets of various sizes are captured and tested from their different vibrational resonances. Additionally, the curves between the diameter, resonance mode number, and vibrational frequency are summarized in Fig. 3(c), which clearly shows a red frequency detuning of the vibrational mode with the same order when increasing the droplet's diameter.

We compare the theoretical curve from the simulation (solid lines with different colors representing different modes) with our experimental data. As can be clearly observed in the figure, the experimental results are in close agreement with the simulation results, although the simulation results are slightly larger than the experimental results in small droplets due to the same thickness of the surface layer. The error may come from the measurement of the water droplet diameter, because the diameter depends on how to measure the pixels of the levitated droplet, such as in different directions. For the same resonance mode number, there is the same integer number of wavelengths on the surface of the droplet, such that the droplet with a larger radius has a lower vibrational frequency. It is also obvious that the high-order mode frequency decreases faster than lower-order modes. We conclude that each vibrational frequency and frequency interval decrease with the increase of the radius of the droplet both in the simulation and in the experiment.

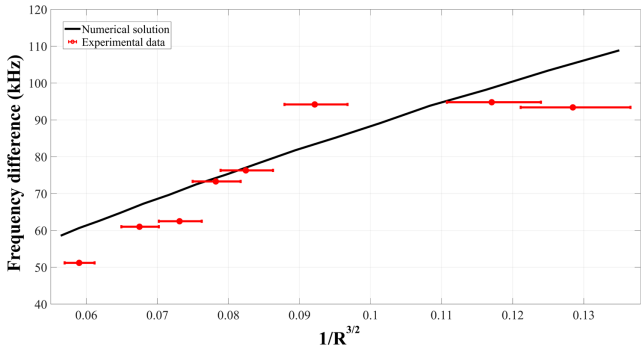

Fig. 4. Frequency difference (first and second mode) dependence to $1/R^{\frac{3}{2}}$ predicted by Sharp's formula. The solid line is a theoretical curve calculated by Sharp's formula, while the dots are experimental data.

Here we can also compare the theoretical relationship between $1/R^{\frac{3}{2}}$ and the frequency difference (first and second mode), as shown in Fig. 4. The frequency difference is linearly correlated with $1/R^{\frac{3}{2}}$ with the root-mean-square error (RMSE) and the correlation coefficient between the simulation curve and experimental data: RMSE = 7.633, $r = 0.877$. Additionally, the error relating to the size of the levitated droplet is about 0.3142 μm (5 pixels), so small droplets have the greater error in Fig. 4. It is well-known that the optical frequency difference/free spectral range is the sophisticated measuring tool to determine the resonant structure's size, e.g., in a Fabry–Perot cavity. Here the frequency difference in the vibrational modes of a droplet can be utilized in the fast measurement of the diameter of the levitated droplet. In the simulation, the n-order resonant mode has $n + 1$ wavelengths, which means that $n + 1$ wavelengths are equal to the circumference. Thus, the frequency difference is strongly sensitive to cavity length and wavelength, and we can use this to measure the circumference of the droplet. Therefore, we propose a suitable and accurate measurement method based on frequency difference, which can be applied in aerosol chemistry for micrometer-sized droplets.

Besides the aforementioned applications in precise metrology in droplet size, as shown in Sharp's formula, other parameters, such as density and surface tension can be retrieved using this new technique. This technique can be applied to determine the aerosol particle's containment information, such as solid remaining, oil concentration, and chemical species [22]. This information is crucial from the environmental perspective. Our technique may provide a non-invasive and *in vivo* alternative

to study these properties in a real-time manner. Additionally, when the higher-order modes are excited with sufficiently large amplitudes, the droplet begins to eject small secondary droplets from the wave crests, which can be used in spray coating, emulsification, and nebulization [34]; these processes may be more feasible with this levitation technique. Moreover, the current experimental setup may also enable optical excitation/cooling of a droplet vibrational mode similar to cooling three spatial degrees of freedom of a single trapped silica nanoparticle in a high vacuum [35]. By implementing active parametric feedback in the optical trap, we can reduce the thermally induced vibration and stabilize the droplet's Brownian motion. Moreover, two or several droplets can be manipulated and coalesced into one droplet by a holographic system with the designed trap pattern [36]. Additionally, the coalescence event can be recorded by the elastic backscattering light from the optical tweezers.

In conclusion, we have demonstrated a levitated droplet by an optical tweezer and that its vibrational modes can be optically excited using the same trapping laser. The observed vibrations are sensitive to the droplet sizes. This experimental configuration can provide an isolated and contact-free environment to levitate a liquid droplet and allow exciting and detecting such vibrational modes in an all-optical fashion, which can be applied in aerosol science and biomedical applications.

Funding. National Natural Science Foundation of China (11304201, 11674228, 92050113); National Key Research and Development Program of China (2016YFA0302500, 2017YFA0303700); Shanghai MEC Scientific Innovation Program (E00075).

Disclosures. The authors declare no conflicts of interest.

Data Availability. Data underlying the results presented in this Letter are not publicly available at this time, but may be obtained from the authors upon reasonable request.

REFERENCES

1. A. Ashkin, Phys. Rev. Lett. **24**, 156 (1970).
2. A. Ashkin and J. Dziedzic, Science **187**, 1073 (1975).
3. T. Li, S. Kheifets, D. Medellin, and M. G. Raizen, Science **328**, 1673 (2010).
4. E. A. Abbondanzieri, W. J. Greenleaf, J. W. Shaevitz, R. Landick, and S. M. Block, Nature **438**, 460 (2005).
5. S. Dumont, W. Cheng, V. Serebrov, R. K. Beran, I. Tinoco, A. M. Pyle, and C. Bustamante, Nature **439**, 105 (2006).
6. K. Svoboda, C. F. Schmidt, B. J. Schnapp, and S. M. Block, Nature **365**, 721 (1993).
7. H. Xin, Y. Li, and B. Li, Adv. Funct. Mater. **25**, 2816 (2015).
8. M. Dao, C. T. Lim, and S. Suresh, J. Mech. Phys. Solids **51**, 2259 (2003).
9. R. Agarwal, K. Ladavac, Y. Roichman, G. Yu, C. M. Lieber, and D. G. Grier, Opt. Express **13**, 8906 (2005).
10. A. Ashkin and J. M. Dziedzic, Appl. Phys. Lett. **19**, 283 (1971).
11. A. A. Geraci, S. B. Papp, and J. Kitching, Phys. Rev. Lett. **105**, 101101 (2010).
12. W. Thomson, London Edinburgh Dublin Philos. Mag. J. Sci. **42**(282), 448 (1871).
13. S. Maayani, L. L. Martin, S. Kaminski, and T. Carmon, Optica **3**, 552 (2016).
14. J. S. Sharp, Soft Matter **8**, 399 (2012).
15. B. Vukasinovic, M. K. Smith, and A. Glezer, J. Fluid Mech. **587**, 395 (2007).
16. H. R. Lamb, *Hydrodynamics*, 6th ed. (Cambridge University, 1993).
17. B. Vukasinovic, M. K. Smith, and A. Glezer, Phys. Fluids **16**, 306 (2004).
18. P. Calvert, Chem. Mater. **13**, 3299 (2001).
19. T. Schneider, J. Kreutz, and D. T. Chiu, Anal. Chem. **85**, 3476 (2013).
20. F. Mugele, J. C. Baret, and D. Steinhauser, Appl. Phys. Lett. **88**, 204106 (2006).
21. P. M. McGuiggan, D. A. Grave, J. S. Wallace, S. Cheng, A. Prosperetti, and M. O. Robbins, Langmuir **27**, 11966 (2011).
22. M. Takahisa, Jpn. J. Appl. Phys. **43**, 6425 (2004).
23. S. Kaminski, L. L. Martin, S. Maayani, and T. Carmon, Nat. Photonics **10**, 758 (2016).
24. J.-Z. Zhang and R. K. Chang, J. Opt. Soc. Am. B **6**, 151 (1989).
25. T. Carmon, H. Rokhsari, L. Yang, T. J. Kippenberg, and K. J. Vahala, Phys. Rev. Lett. **94**, 223902 (2005).
26. M. Tomes and T. Carmon, Phys. Rev. Lett. **102**, 113601 (2009).
27. J. Yang, Q. Tian, F. Zhang, X. Chen, X. Jiang, and W. Wan, Nanophotonics **9**, 2915 (2020).
28. G. Bahl, K. H. Kim, W. Lee, J. Liu, X. Fan, and T. Carmon, Nat. Commun. **4**, 1994 (2013).
29. K. H. Kim, G. Bahl, W. Lee, J. Liu, M. Tomes, X. Fan, and T. Carmon, Light Sci. Appl. **2**, e110 (2013).
30. D. R. Burnham and D. McGloin, Opt. Express **14**, 4175 (2006).
31. R. Dahan, L. L. Martin, and T. Carmon, Optica **3**, 175 (2016).
32. J. Zehnpfennig, G. Bahl, M. Tomes, and T. Carmon, Opt. Express **19**, 14240 (2011).
33. "COMSOL multiphysics," 2021, https://comsol.com/.
34. M. K. Smith, B. Vukasinovic, and A. Glezer, 4th Microgravity Fluid Physics and Transport Phenomena Conference, Cleveland, Ohio, USA (1998), p. 447.
35. J. Gieseler, B. Deutsch, R. Quidant, and L. Novotny, Phys. Rev. Lett. **109**, 103603 (2012).
36. B. Bzdek, L. Collard, J. E. Sprittles, A. J. Hudson, and J. P. Reid, J. Chem. Phys. **145**, 054502 (2016).